

# Measurement of $T_1$ relaxation rates of natural abundant $^{13}\text{C}$ at C2' in a non-uniformly deuterium-labelled oligo-DNA



T. V. Maltseva, A. Földesi and J. Chattopadhyaya\*

Department of Bioorganic Chemistry, Box 581, Biomedical Center, Uppsala University, S-751 23 Uppsala, Sweden. E-mail: jyoti@bioorgchem.uu.se; Fax: +4618554495

Received (in Cambridge) 21st July 1998, Accepted 23rd October 1998

The  $T_1$  relaxation rate of C2' at natural abundance of four different stereoselectively C2' deuterio-labelled nucleotide residues [ $2'$ - $^2\text{H}$  (S):  $\sim 85$  atom%  $^2\text{H}$ ;  $2''$ - $^2\text{H}$  (R):  $\sim 15$  atom%  $^2\text{H}$ ;  $3'$ - and  $5'/5''$ - $^2\text{H}$ :  $>97$  atom%  $^2\text{H}$ ;  $4'$ - $^2\text{H}$ :  $\sim 65$  atom%  $^2\text{H}$ ] in duplex I,  $\text{d}^5(\text{C}^2\text{G}^3\text{C}^4\text{G}^5\text{A}^6\text{T}^7\text{T}^8\text{C}^{10}\text{G}^{11}\text{C}^{12}\text{G})_2^3$ , (1.13 mM) has been measured for the first time. Only the  $^{13}\text{C}$  nuclei bearing both proton and deuterium have been detected by  $^1\text{H}$ - $^{13}\text{C}$  2D heteronuclear experiments by filtering away all other methylene  $^{13}\text{C}$  nuclei. A similar experiment performed without deuterium decoupling allows the observation of  $^{13}\text{C}(2')$ - $^2\text{H}$  coupling, which semiquantitatively gives information regarding the dynamics of 2'-methylene fragments in deuterated DNA duplex II with natural  $^{13}\text{C}$  abundance,  $\text{d}^5(\text{C}^2\text{G}^3\text{C}^4\text{G}^5\text{A}^6\text{T}^7\text{T}^8\text{C}^{10}\text{G}^{11}\text{C}^{12}\text{G})_2^3$ , at 2.5 mM concentration [ $2'$ - $^2\text{H}$  (S):  $\sim 85$  atom%  $^2\text{H}$ ;  $2''$ - $^2\text{H}$  (R):  $\sim 15$  atom%  $^2\text{H}$ ;  $3'$ - $^2\text{H}$ :  $>97$  atom%  $^2\text{H}$ ;  $5'$ - $^2\text{H}/5''$ - $^2\text{H}$  (R/S)  $\sim 50:50$  atom%  $^2\text{H}$ ]. It is noteworthy that despite the concentration increase of duplex II over duplex I by two-fold, only  $^{13}\text{C}(2')$ - $^2\text{H}$  coupling was observable for the former but not the  $^{13}\text{C}(5')$ - $^2\text{H}$  coupling because of the sensitivity problem owing to the proximity of C5' to the water resonance.

## Introduction

The development of chemoselective approaches for incorporation of deuterium  $^1$  in nucleoside residues has paved the way for selective non-uniform labelling of oligo-DNA and RNA with these building blocks at specific sites of interest. The non-uniform deuterium labelling (*i.e.* the "NMR-window" approach)<sup>1a-g</sup> has been developed in our laboratory to aid the assignment problem of the overlapping NMR resonances in large oligo-DNA and RNA, which is one of the most serious problems encountered in the elucidation by NMR of their structure. Based on this concept, the solution structures of 21mer<sup>1f</sup> and 31mer oligo-RNAs<sup>1g</sup> have been solved. It has been<sup>1e</sup> shown that the deuteration helps to determine the  $^3J_{\text{HH}}$  couplings of the backbone and sugar moieties for deoxyoligonucleotides of up to 40 nucleotide residues<sup>1e,2,3</sup> by elimination of large H2'-H2'' and H5'-H5'' geminal coupling constants. It also decreases the effect of spin-diffusion,<sup>1e</sup> and increases the number of nOe constraints<sup>1e,2</sup> in the structure elucidation of the oligo-DNA.

Dynamic studies of oligo-DNA have mainly been carried out by deuterium relaxation measurements in the solid state.<sup>4</sup> A few dynamic studies<sup>5</sup> in solution based on the measurement of the relaxation rate of the  $^{13}\text{C}$  nucleus have been performed on oligo-DNA with naturally abundant  $^{13}\text{C}$ . These studies have shed light<sup>5</sup> on how the structure and dynamics of small or middle-sized DNA molecules are actually perturbed by interaction with various ligands or drugs.<sup>5a</sup> These earlier studies have been restricted to relaxation measurements of the methine-carbons such as C1', C3' and C4'. One of the serious bottlenecks of these studies is however that they can be performed only for small molecules because of the severe spectral overlap encountered in the larger oligonucleotides.

We herein demonstrate for the first time that specific incorporation of the diastereoselectively deuterium-labelled 2'-deoxynucleoside blocks indeed makes it possible to measure the  $T_1$  relaxations of those 2'-partially-deuterated methylene carbons at natural abundance in an oligo-DNA at 1.13 mM duplex concentration due to reduced spectral overlap. Moreover, we demonstrate that for diastereoselectively deuterated  $^1\text{H}$ - $^{13}\text{C}(2')$ - $^2\text{H}$  at natural abundant  $^{13}\text{C}$ , it is experimentally

possible to observe the shape and splitting pattern of  $^{13}\text{C}$  attached to  $^2\text{H}$ ,<sup>6a-d</sup> which can potentially be useful for numerical simulation to extract<sup>6d-f</sup> spectral density function parameters. Thus, this work can potentially provide unique information about the overall and internal correlation times and the order parameters of the sugar moieties of oligo-DNA.

## Materials and methods

### NMR sample preparation

$2'(R/S),3',5'(R/S)$ - $d_3$ -2'-deoxynucleosides [ $2'$ - $^2\text{H}$  (S):  $\sim 85$  atom%  $^2\text{H}$ ;  $2''$ - $^2\text{H}$  (R):  $\sim 15$  atom%  $^2\text{H}$ ;  $3'$ - $^2\text{H}$ :  $>97$  atom%  $^2\text{H}$ ;  $5'$ - $^2\text{H}/5''$ - $^2\text{H}$  (R/S)  $\sim 50:50$  atom%  $^2\text{H}$ ] and  $2'(R/S),3',4',5',5''$ - $d_5$ -2'-deoxynucleosides [ $2'$ - $^2\text{H}$  (S):  $\sim 85$  atom%  $^2\text{H}$ ;  $2''$ - $^2\text{H}$  (R):  $\sim 15$  atom%  $^2\text{H}$ ;  $3'$ - and  $5'$ - $^2\text{H}$ :  $>97$  atom%  $^2\text{H}$ ;  $4'$ - $^2\text{H}$ :  $\sim 65$  atom%  $^2\text{H}$ ] were obtained by methods described by us earlier.<sup>1e</sup> The duplex I,  $\text{d}^5(\text{C}^2\text{G}^3\text{C}^4\text{G}^5\text{A}^6\text{T}^7\text{T}^8\text{C}^{10}\text{G}^{11}\text{C}^{12}\text{G})_2^3$ , contains selectively incorporated  $2'(R/S),3',4',5',5''$ - $d_5$ -2'-deoxynucleoside residues at positions shown by underlining. The duplex II,  $\text{d}^5(\text{C}^2\text{G}^3\text{C}^4\text{G}^5\text{A}^6\text{T}^7\text{T}^8\text{C}^{10}\text{G}^{11}\text{C}^{12}\text{G})_2^3$ , has uniformly incorporated  $2'(R/S),3',5'(R/S)$ - $d_3$ -2'-deoxynucleosides.<sup>2</sup> Both duplexes I and II were prepared by standard phosphoramidite chemistry on the solid phase. Purified samples ( $\sim 1.13$  mM for duplex I and 2.5 mM for duplex II) were dissolved in 0.6 ml of the following buffer for NMR measurements: 100 mM NaCl, 10 mM  $\text{NaH}_2\text{PO}_4$ , 10  $\mu\text{M}$  EDTA, pH 7.0 in  $\text{D}_2\text{O}$ .

### NMR experiments

The NMR experiments were carried out on Bruker DRX spectrometers at magnetic field strength 14.1 T, operating at 600.13 MHz for  $^1\text{H}$ , 242.93 MHz for  $^{31}\text{P}$ , 150.91 MHz for  $^{13}\text{C}$  and 92.12 MHz for  $^2\text{H}$ , and at magnetic field strength of 11.7 T operating at 500.03 MHz for  $^1\text{H}$ , 125.74 MHz for  $^{13}\text{C}$  and 76.76 MHz for  $^2\text{H}$ . Both spectrometers were equipped with a Bruker digital lock and with a switching  $^2\text{H}$  lock- $^2\text{H}$  pulse device. The 600.13 MHz spectrometer was equipped with an inverse triple-resonance probehead for  $^1\text{H}$ ,  $^{13}\text{C}$  and  $^{31}\text{P}$  (TXI).  $^1\text{H}$ ,  $^{13}\text{C}$  and  $^{31}\text{P}$  pulses on this probehead were applied with a 31.7, 17.2 and 15.4 kHz field strengths, respectively.  $^{13}\text{C}$  and  $^{31}\text{P}$

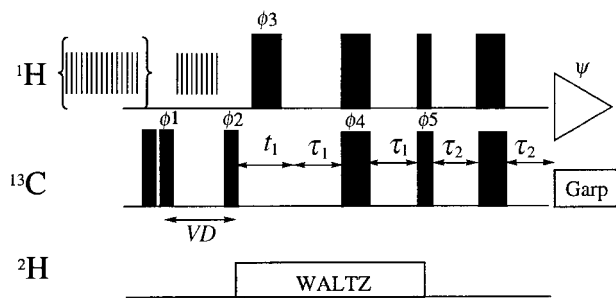


**Fig. 1** The pulse sequence employed for the measurements of  $T_1$  of the  $^{13}\text{C}$  nucleus was implemented with a TXO probe. In this sequence, narrow and wide boxes indicate  $90^\circ$  and  $180^\circ$  pulses, respectively, and unless otherwise indicated, all pulses are applied along the  $x$ -axis. The values of  $\tau_1$  and  $\tau_2$  were set to 1.79 ms [ $\sim 1/(4J_{\text{CH}})$  with  $J_{\text{CH}} = 140$  Hz]. WALTZ decoupling<sup>7b</sup> of  $^2\text{H}$  during pulsing was achieved using a 1.3 kHz field. GARP<sup>7a</sup> decoupling of  $^{13}\text{C}$  during acquisition was achieved using a 4.17 kHz field strength. Phase cycling used in experiments is  $\phi_1 = x, -x$ ;  $\phi_2 = x$ ;  $\phi_3 = 8(x), 8(-x)$ ;  $\phi_4 = 2(x), 2(y), 2(-x), 2(-y)$ ;  $\phi_5 = 8(y), 8(-y)$ ; and receiver is  $\psi = 2(x, -x, -x, x), 2(-x, x, x, -x)$ . Quadrature detection in the F1 dimension was achieved with TPPI on  $\phi_2$ . Weak presaturation of the solvent was used. The cascades of  $135^\circ$  proton pulses have been applied with repetition rates of 5 ms during 1.5 s in prescan delay and relaxation delay  $VD$ .

decoupling were performed using GARP<sup>7a</sup> with 4.17 and 1.79 kHz field strengths. For the  $90^\circ$  and  $180^\circ$   $^2\text{H}$  pulses the probe power after the switching block was 6.4 W which corresponds to a 2.08 kHz applied field.  $^2\text{H}$  decoupling utilised a WALTZ16<sup>7b</sup> sequence using a 625 Hz field.

The 500.03 MHz spectrometer was equipped with a triple-resonance selective probehead for  $^{13}\text{C}$  and  $^2\text{H}$  (TXO).  $^1\text{H}$  and  $^{13}\text{C}$  pulses were applied with a 24 and 40 kHz field, respectively. This strength of  $^{13}\text{C}$  pulses allowed us to excite the region between  $^{13}\text{C}(5')$  and  $^{13}\text{C}(2')$  resonances and neglected the offset effect on measurement of  $T_1$  relaxation of  $^{13}\text{C}$  as we have shown earlier in our relaxation study on deuterated nucleosides.<sup>3</sup>  $^{13}\text{C}$  decoupling was performed using GARP with a 4.17 kHz field strength. For the  $90^\circ$  and  $180^\circ$   $^2\text{H}$  pulses, the probehead power after the switching block was 43.0 W which corresponds to an 11.4 kHz applied field.  $^2\text{H}$  decoupling utilised a WALTZ16 sequence using a 1.3 kHz field (0.6 W).

To avoid the spinning artifacts, all spectra were measured on non-spinning samples.

The experimental conditions for standard HSQC<sup>8</sup> experiments with deuterium or phosphorus decoupling are listed in the legends of figures. Apodisation, zero-filling and Fourier transformation led to a digital resolution of 1.03 Hz/point in the F1 and 2.93 Hz/point in the F2 dimension for experiments with  $SW(^{13}\text{C}) = 28$  ppm and 4.91 Hz/point in the F1 and 2.44 Hz/point in the F2 dimension for experiments with  $SW(^{13}\text{C}) = 80$  ppm.

**The determination of  $T_1$  relaxation time of  $^{13}\text{C}$  in the  $^1\text{H}$ - $^{13}\text{C}(2')$ - $^2\text{H}$  fragment by 2D experiment.** Fig. 1 shows the pulse sequence used to record  $^{13}\text{C}$   $T_1$  values originally proposed by Kay<sup>9</sup> with the only difference being that during  $^{13}\text{C}$  chemical shift evolution in the  $t_1$  period, followed by a reverse INEPT transfer step from  $^{13}\text{C}$  to  $^1\text{H}$ , the WALTZ16 modulation<sup>7b</sup> on deuterium was used to decouple  $^{13}\text{C}$  from deuterium. The train of  $^1\text{H}$   $125^\circ$  pulses was applied every 5 ms before inversion and during recovery of the  $^{13}\text{C}$  magnetisation in the same way as proposed<sup>9</sup> to minimise the effects of cross-relaxation and from intramolecular dipolar and CSA cross-correlation. The data sets were recorded as a  $4\text{K} \times 128$  real matrix with 512 scans for  $^{13}\text{C}$  relaxation measurement for each  $t_1$  value and a spectral width of 10 ppm in F2 and 100 ppm in F1 with the carrier for  $^1\text{C}$ ,  $^{13}\text{C}$ ,  $^2\text{H}$  at 4.8, 50 and 4.8 ppm, respectively.

**Data evaluation in 2D experiments.** The spectra were processed and analysed on a Silicon Graphics workstation using

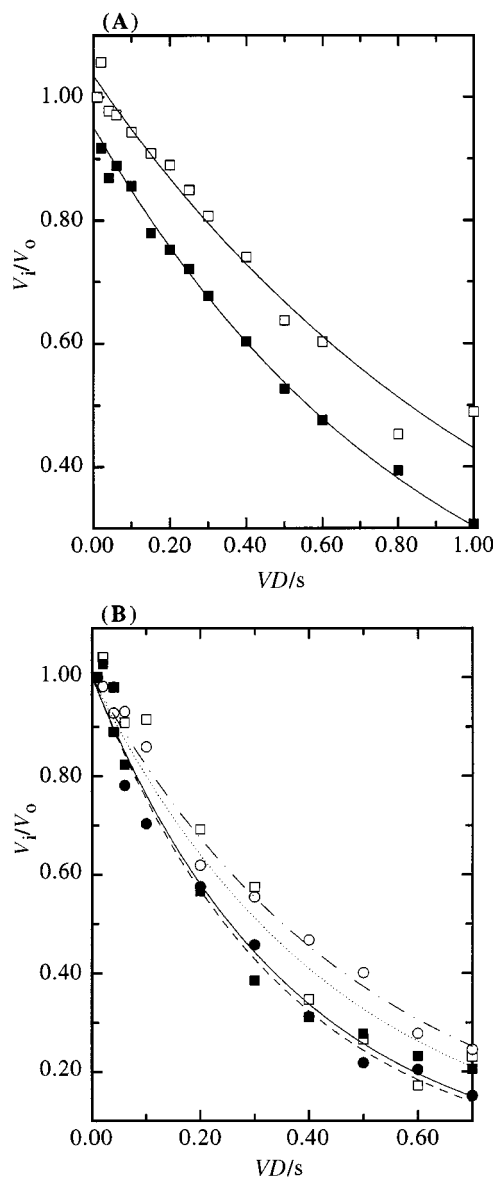


**Fig. 2** Panel A shows the normalised  $T_1$  decay curves of  $^{13}\text{C}$  nuclei at natural abundance for  $2'(R/S),3',5'(R/S)$ - $d_3$ -thymidine (30 mg in 0.6 ml of  $\text{D}_2\text{O}$ ) and Panel B shows for selectively deuterated oligo-DNA [*i.e.*  $d^5(1^2\text{C}^2\text{G}^3\text{C}^4\text{G}^5\text{A}^6\text{T}^7\text{C}^8\text{G}^9\text{C}^{10}\text{G}^{11}\text{C}^{12}\text{G})_2$ ], duplex I] with deuterated  $^3\text{C}$ ,  $^5\text{A}$ ,  $^8\text{T}$  and  $^{10}\text{G}$  nucleotides, obtained from the volume of cross-peaks in  $^1\text{H}$ - $^{13}\text{C}$  2D correlation spectra (see Fig. 1) ( $NS = 128$  and 512) as a function of relaxation delay,  $VD$ . In Panel A, the experimental data points (experiments with 14 different relaxation delays have been performed) are marked by (■) for  $^{13}\text{C}(2')$  and by (□) for  $^{13}\text{C}(4')$  nuclei. In Panel B, the experimental data points for  $^{13}\text{C}(2')$  nuclei of deuterated  $^3\text{C}$ ,  $^5\text{A}$ ,  $^8\text{T}$  and  $^{10}\text{G}$  nucleotides are marked by (○), (□), (●) and (■) symbols, respectively, with 12 different relaxation delays. The curves show the best-fits to single-exponential decays. The corresponding datasets are listed in Table 1.

XWINNMR v. 2.1 and AURELIA programs (BRUKER). Apodisation, zero-filling and Fourier transformation led to a digital resolution of 12.27 Hz/point in the F1 and 1.22 Hz/point in the F2 dimension. For the evaluation of the  $T_1$  relaxation time the volumes of cross-peaks in the series of 2D spectra (Fig. 1) were fitted to a single exponential, depending on the relaxation delay using eqn. (1), where  $T_1$  is the relaxation rate,

$$V(A) = V(0)\exp(-A/T_1) \quad (1)$$

$V(A)$  and  $V(0)$  are the volumes of cross-peaks at time  $A$  (defined in Fig. 1 as  $VD$ ) and zero time.

The fit (Fig. 2) was performed using a least squares minimisation procedure using program PROFIT 4.2. The mono-

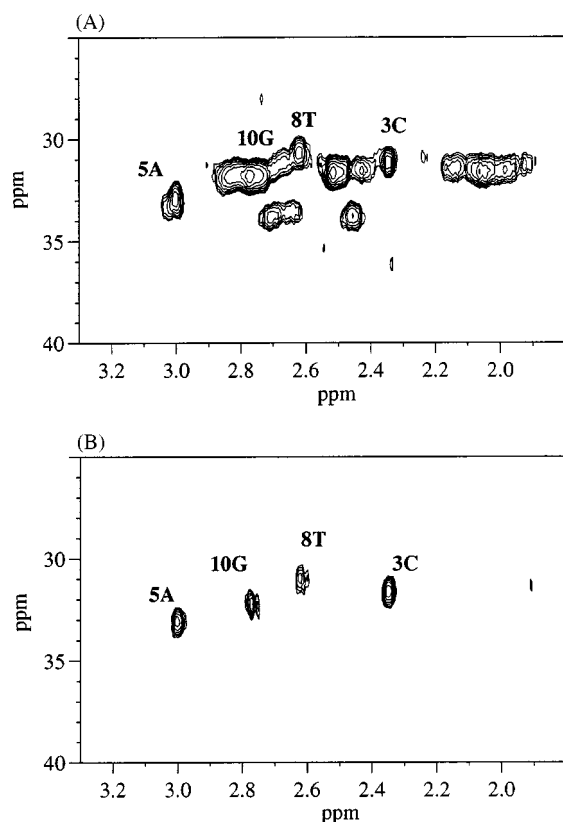


**Fig. 3** Comparison of standard  $^1\text{H},^{13}\text{C}$ -HSQC spectra with deuterium decoupling (Panel A) with the  $^1\text{H},^{13}\text{C}$  correlation spectra (Panel B) using the pulse sequence in Fig. 1 of duplex **I**,  $\text{d}^5(\text{C}^2\text{G}^3\text{C}^4\text{G}^5\text{A}^6\text{T}^7\text{T}^8\text{C}^9\text{G}^{10}\text{C}^{11}\text{C}^{12}\text{G})_2^3$ , with deuterated  $^3\text{C}$ ,  $^5\text{A}$ ,  $^8\text{T}$  and  $^{10}\text{G}$  nucleotides at  $^{13}\text{C}$  in natural abundance. Both Panels A and B show the  $\text{H}2'/\text{H}2''\text{-}^{13}\text{C}(2')$  region. In Panel B all four  $\text{H}2''\text{-}^{13}\text{C}(2')$  cross-peaks are clearly observed; they are marked by residue number. In Panel A, the  $\text{H}2''\text{-}^{13}\text{C}(2')$  area is crowded because of the presence of all  $\text{H}2'\text{-}^{13}\text{C}(2')$  and  $\text{H}2''\text{-}^{13}\text{C}(2')$  cross-peaks in duplex **I**. The total measurement time of the standard  $^1\text{H},^{13}\text{C}$ -HSQC experiment was  $\sim 18$  h:  $256 \times 2\text{K}$  complex  $t_1$  and  $t_2$  points were acquired with acquisition times of 0.029 and 0.103 s, respectively, with 128 scans; the sweep width of the  $^{13}\text{C}$  dimension was 180 ppm with the carrier for  $^{13}\text{C}$  at 71.6 ppm. The total measurement time of the  $^1\text{H},^{13}\text{C}$  experiment in Panel B was  $\sim 44$  h:  $128 \times 2\text{K}$  complex  $t_1$  and  $t_2$  points were acquired with acquisition times of 0.003 and 0.205 s, respectively, with 512 scans; the sweep width of the  $^{13}\text{C}$  dimension was 100 ppm with the carrier for  $^{13}\text{C}$  at 50.0 ppm. The experiment was carried out with  $VD = 10$  ms (see Fig. 1). WALTZ decoupling<sup>7b</sup> of  $^2\text{H}$  during pulsing was achieved using a 1.3 kHz field.

exponential character of decay was tested using Monte Carlo procedures as established in the literature.<sup>10</sup>

## Results and discussion

(A) Two expanded plots of the  $^1\text{H}(2')/\text{H}(2'')\text{-}^{13}\text{C}(2')$  region of two  $^1\text{H}\text{-}^{13}\text{C}$  correlation experiments are presented in Fig. 3. Panel A shows the standard HSQC<sup>8</sup> experiment [*i.e.* Fig. 3(A)], whereas Panel B [*i.e.* Fig. 3(B)] shows the spectrum as a result of spectral editing<sup>11</sup> performed with the pulse sequence shown in Fig. 1 for selectively deuterated oligo-DNA duplex **I** [*i.e.*  $\text{d}^5(\text{C}^2\text{G}^3\text{C}^4\text{G}^5\text{A}^6\text{T}^7\text{T}^8\text{C}^9\text{G}^{10}\text{C}^{11}\text{C}^{12}\text{G})_2^3$ , with deuterated  $^3\text{C}$ ,  $^5\text{A}$ ,  $^8\text{T}$  and  $^{10}\text{G}$  nucleotide residues]. All  $2'$ -carbons in duplex **I** are visible in Fig. 3(A) as well as the intractable spectral overlap. The experiment in Fig. 3(B), however, allows us to successfully select only those  $^1\text{H}\text{-}^{13}\text{C}(2')$  cross-peaks resulting from partially-deuterated  $\text{C}2'$  which has both proton and deuterium (85 atom%  $^2\text{H}$ ) covalently bonded to it (*i.e.* only the partially-deuterated  $\text{C}2'$  methylene-carbons in  $^3\text{C}$ ,  $^5\text{A}$ ,  $^8\text{T}$  and  $^{10}\text{G}$  nucleotide residues in duplex **I**) and exclude the  $2'$  and  $5'$  protonated methylene-carbons from the non-deuterated nucleotide residues in duplex **I**.

**Table 1** Longitudinal ( $T_1$ ) relaxation times for  $^{13}\text{C}(2')$  for four deuterated residues of duplex **I** and for  $2'(R/S),3',5'(R/S)\text{-d}_3\text{-thymidine}$  at 11.7 T at 298 K (TXO probe)

Compound	Type of carbon nucleus	$T_1/\text{s}$
Duplex <b>I</b>	$^3\text{C}(2')$	$0.44 \pm 0.04^a$
	$^5\text{A}(2')$	$0.51 \pm 0.02^a$
	$^8\text{T}(2')$	$0.36 \pm 0.02^a$
	$^{10}\text{G}(2')$	$0.35 \pm 0.02^a$
$2'(R/S),3',5'(R/S)\text{-d}_3\text{-thymidine}$	$^{13}\text{C}(2')(^2\text{H},^1\text{H})$	$1.14 \pm 0.06^a$ $(1.10 \pm 0.03)^b$
	$^{13}\text{C}(4')(^1\text{H})$	$0.87 \pm 0.03^a$ $(0.87 \pm 0.05)^b$

<sup>a</sup> Data obtained using 2D experiment using the pulse program as shown in Fig. 1. <sup>b</sup> Data obtained using 1D inversion recovery experiment.

(B) The experiment presented in Fig. 3(B) allows us to perform the relaxation time measurement of  $^{13}\text{C}$  nuclei of partially deuterated-methylene fragments of nucleotide residues bearing diastereomeric proton and deuterium. We herein have illustrated the sensitivity of this experiment by performing the  $T_1$  measurement of  $^{13}\text{C}$  at natural abundance with a 1.13 mM duplex in 0.6 ml of deuterium oxide. The decays of volume of  $^{13}\text{C}(2')\text{-H}2'$  cross-peaks for four  $^3\text{C}$ ,  $^5\text{A}$ ,  $^8\text{T}$  and  $^{10}\text{G}$  nucleotide residues of dodecamer **I** versus the relaxation delays ( $VD$ ) are shown in Fig. 2(B), and Table 1 shows the resulting  $T_1$  data. For comparison, the decays of volume of  $^{13}\text{C}(2')\text{-H}2'$  and  $^{13}\text{C}(4')\text{-H}4'$  cross-peaks from  $2'(R/S),3',5'(R/S)\text{-d}_3\text{-thymidine}$  (30 mg in 0.6 ml of deuterium oxide) are presented [Fig. 2(A)]. The longitudinal relaxation times for  $2'(R/S),3',5'(R/S)\text{-d}_3\text{-thymidine}$  are listed in Table 1 together with data obtained from the 1D version of the inversion recovery experiment. Comparison of these data shows that the  $T_1$  relaxation times obtained by the 2D method are well within the experimental error ( $\pm 5\%$ )<sup>3</sup> for data obtained from conventional inversion recovery experiments.

Our earlier studies<sup>3</sup> have shown the influence of deuterium on the  $T_1$  and  $T_2$  relaxation of  $^{13}\text{C}$  in fully-deuterated  $3'$ -methylene and partially-deuterated methylene ( $^1\text{H}\text{-}^{13}\text{C}\text{-}^2\text{H}$  at  $2'$  and  $5'$  positions) fragments using selectively  $^2\text{H}$  labelled nucleoside blocks [ $2'(R/S),3',5'(R/S)\text{-d}_3\text{-nucleosides}$ ] with natural  $^{13}\text{C}$  abundance. It was found<sup>3,6a-d,12</sup> that the quadrupolar- $\text{dd}(^{13}\text{C}\text{-}^2\text{H})$  cross-relaxation only strongly participates in the transverse relaxation rate of  $^{13}\text{C}$  of deuterated-methylene type carbons. It was also found to be possible to extract pure dipole-dipole  $T_1$  and  $T_2$  terms of  $^{13}\text{C}$  of methylene ( $^1\text{H}\text{-}^{13}\text{C}\text{-}^2\text{H}$ ) groups in a sugar moiety of a nucleoside residue since the effects of dipole-dipole cross-correlation between  $^1\text{H}\text{-}^{13}\text{C}$  and  $^2\text{H}\text{-}^{13}\text{C}$  groups are smaller than in the  $^{13}\text{C}(^1\text{H})_2$  spin system.<sup>13</sup>

(C) Another application of deuterated nucleoside with natural abundance carbon is based on the analysis of the shape of  $^1\text{H}\text{-}^{13}\text{C}(2')$  cross-peaks to estimate  $^3J_{\text{H}1\text{-}^{13}\text{C}(2')}$  coupling constants. In Fig. 4(A), the folding<sup>14</sup> HSQC experiment with  $^2\text{H}$  decoupling on duplex **II**,  $\text{d}^5(\text{C}^2\text{G}^3\text{C}^4\text{G}^5\text{A}^6\text{T}^7\text{T}^8\text{C}^9\text{G}^{10}\text{C}^{11}\text{C}^{12}\text{G})_2^3$  [all natural nucleosides are replaced with  $2'(R/S),3',5'(R/S)\text{-d}_3\text{-}2'$ -deoxynucleosides], is presented. In addition to the obvious benefits such as the elimination of geminal coupling constants in the sugar moiety<sup>16,2</sup> for accurate determination of vicinal coupling constants ( $^3J_{\text{H}1'\text{H}2'}$ ,  $^3J_{\text{H}1'\text{H}2''}$ ,  $^3J_{\text{H}4'\text{H}5'}$  and  $^3J_{\text{H}4'\text{H}5''}$ ), the increases of intensities of  $^1\text{H}\text{-}^{13}\text{C}(2')$  cross-peaks are clearly observed in Fig. 4(A). This experiment also provides a unique opportunity for the determination of the  $^3J_{\text{H}1\text{-}^{13}\text{C}(2')}$  coupling constant which is very important for distinguishing between  $\text{B}_I$  and  $\text{B}_{II}$  types of sugar conformation of DNA.<sup>15</sup> Our data show that the  $^3J_{\text{H}1\text{-}^{13}\text{C}(2')}$  coupling constants for the Dickerson-Drew dodecamer **II** investigated in this work are well below the linewidth of cross-peaks in the F1

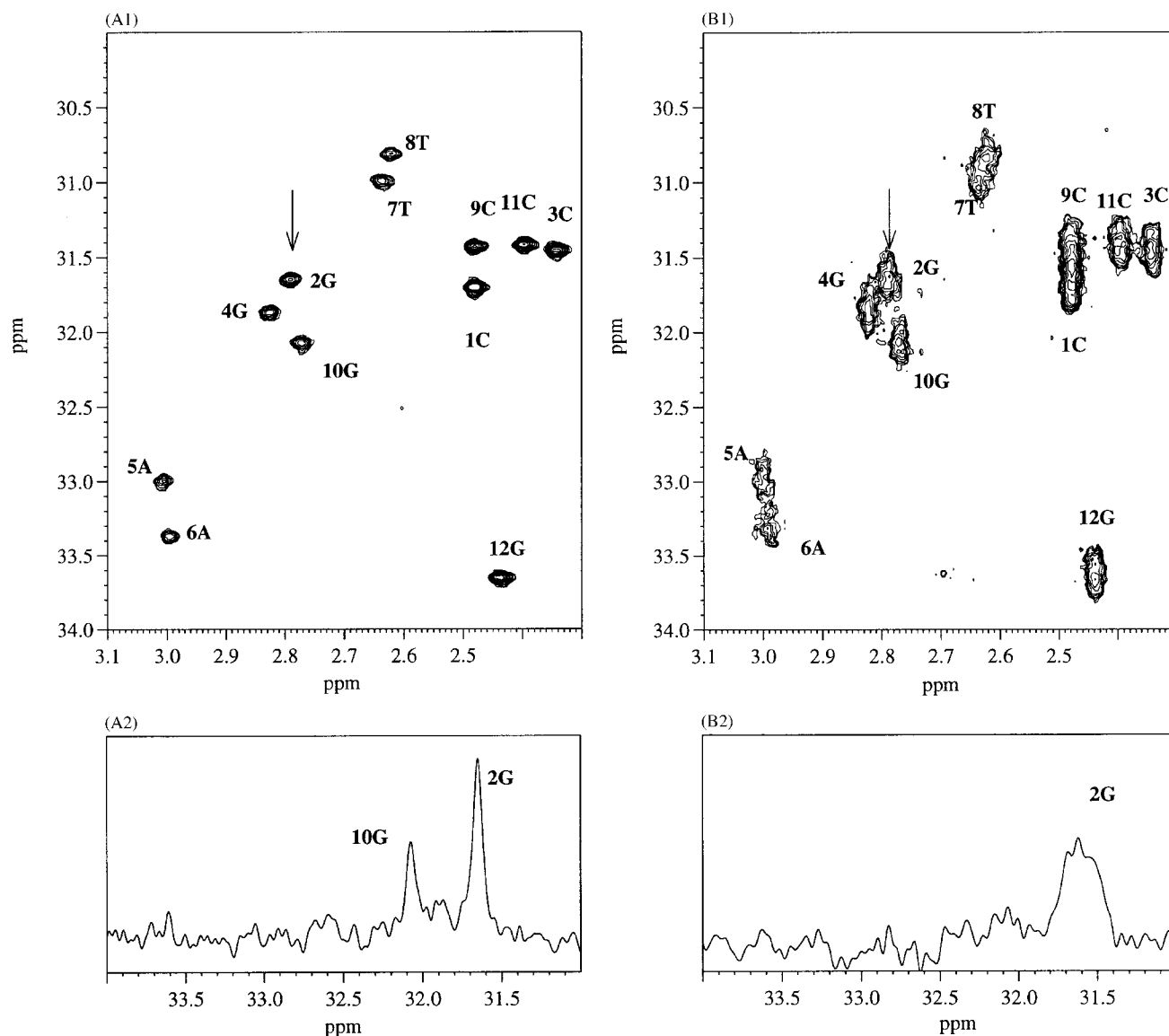


**Fig. 4** Comparison of the standard  $^1\text{H}$ ,  $^{13}\text{C}$ -HSQC spectra with deuterium decoupling (Panels A) and without deuterium decoupling (Panels B) of deuterated duplex II,  $d^5(1^2\text{C}^2\text{G}^3\text{C}^4\text{G}^5\text{A}^6\text{A}^7\text{T}^8\text{T}^9\text{C}^{10}\text{G}^{11}\text{C}^{12}\text{G})_2^{3'}$ , with  $^{13}\text{C}$  at natural abundance. Both Panels A and B show the  $\text{H}2'/\text{H}2''$ - $^{13}\text{C}(2')$  region, but only the  $\text{H}2''$ - $^{13}\text{C}(2')$  cross-peaks are observed (marked by residue number) because  $\text{H}2'$  has been replaced by  $^2\text{H}$  in all  $2'(R/S), 3', 5'(R/S)$ - $d_3$ - $2'$ -deoxynucleosides. The total measurement time was  $\sim 18$  h:  $1292 \times 4\text{K}$  complex  $t_1$  and  $t_2$  points were acquired with acquisition times of 0.077 and 0.170 s, respectively. The number of scans was 128 and 256, respectively. Both HSQC experiments were performed with extensive folding<sup>14</sup> in the F1 dimension: the sweep width of the  $^{13}\text{C}$  dimension was 28 ppm with the carrier for  $^{13}\text{C}$  at 38 ppm in the  $^{13}\text{C}(2')$  region. The experiments were carried out at a magnetic field strength of 14.1 T. WALTZ decoupling<sup>7b</sup> of  $^2\text{H}$  (or  $^{31}\text{P}$ ) during pulsing was achieved using a 625 Hz (or 1.785 kHz) field. The projection through the  $\text{H}2''$ - $^{13}\text{C}(2')$  cross-peak in the F1 dimension has been shown, only as an example, for the  $^2\text{G}$  residue (a part of the signal of the  $^{10}\text{G}$  residue is also seen) in Panel A1 in deuterium decoupled mode showing that the pseudosinglets for  $^3J_{\text{H}2''\text{C}(2')}$  are visible because this coupling constant is less than the linewidth of the resonance ( $< 2$  Hz). It is noteworthy that similar pseudosinglets have been observed for all nucleotide residues suggesting a  $\text{B}_1$ -type conformation for the phosphate backbone for duplex I. In Panel B2, there is only  $^{31}\text{P}$  decoupling applied (no deuterium decoupling), thereby allowing us to observe the  $^{13}\text{C}(2')$ - $^2\text{H}$  splitting in the methylene triplet for the  $^2\text{G}$  residue.

dimension ( $< 2$  Hz) which correspond to the  $\text{B}_1$  type conformation<sup>15</sup> of DNA for all residues.

(D) Recent numerical simulations<sup>6e,f</sup> (which are also experimentally validated<sup>6</sup>) of the shape of the  $^{13}\text{C}$ - $^2\text{H}$  methine-triplet at isotropic rotation correlation times ranging from 10 ps to 500 ns have shown its coalescence into a singlet at the  $T_1$ -minimum (at a  $\tau_R \sim 1$ –3 ns), followed by the appearance of the asymmetry of the triplet at correlation times longer than the  $T_1$ -minimum.<sup>6</sup> The asymmetric multiplet patterns observed are shown<sup>6,12</sup> to arise from the dynamic frequency shift. Recently, the effects of the internal motion on the predicted lineshape have also been considered theoretically.<sup>6f</sup> It was concluded<sup>6f</sup> that increasing the disorder of a molecule causes a reduction of the multiplet asymmetry as well as sharper component lines of the multiplet.

In our work (Fig. 5), we have performed a series of

temperature-dependent 1D  $^{13}\text{C}$  experiments on  $2'(R/S), 3', 5'(R/S)$ - $d_3$ -thymidine in a mixture of deuterium oxide and ethylene glycol (1:1, v/v) with overall correlation times ( $\tau_R$ ) ranging from 0.5 to 12.5 ns (see the legend of Fig. 5). It is clear from Fig. 5 that the  $\text{C}2'$ ,  $\text{C}3'$  and  $\text{C}5'$  triplets have collapsed at different temperatures, showing that the dynamics in  $2'(R/S), 3', 5'(R/S)$ - $d_3$ -thymidine are indeed variable [the  $^{13}\text{C}(3')$  methine-carbon has collapsed at  $T \approx 273$  K, whereas  $^{13}\text{C}(2')$  and  $^{13}\text{C}(5')$  methylene-type carbons have collapsed at  $T \approx 278$  K]. The overall  $\tau_R$  for thymidine thus corresponds to  $\sim 3.5$ – $4.4$  ns between 273–278 K. For a correlation time of 1 ns (at 308 K) the symmetrical triplet is clearly observed for all three types of carbons, and the appearance of triplet asymmetry for correlation times longer than the  $T_1$ -minimum is not detectable even at  $\tau_R > 12.5$  ns. This phenomenon could be attributed to

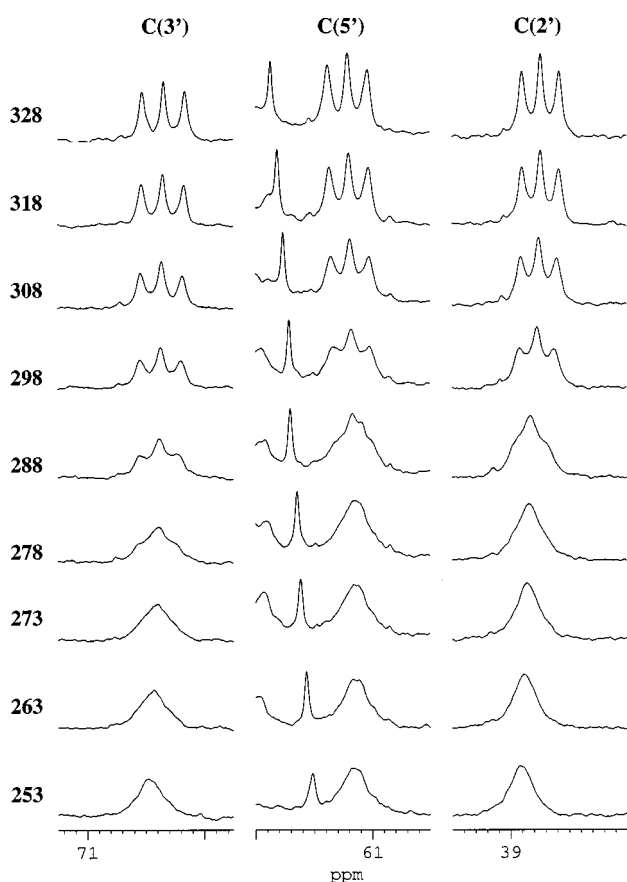


**Fig. 5** 1D  $^{13}\text{C}$  spectra at natural abundance with proton decoupling of 2'(R/S),3',5'(R/S)- $d_3$ -thymidine (30 mg in 0.6 ml of 50% deuterium oxide and 50% ethylene glycol) at various temperatures (indicated on the left side of the spectra) are shown at a magnetic field strength of 11.7 T. Three different spectral regions for the methine triplet of  $^{13}\text{C}(3')$ , and the methylene triplet of  $^{13}\text{C}(5')$  and  $^{13}\text{C}(2')$  from 253 to 328 K are also shown. The overall correlation times obtained from  $T_1$  and  $T_2$  relaxation data of  $^2\text{H}$  (details will be published elsewhere) are respectively as follows: 12.5, 7.3, 4.4, 3.5, 2.2, 1.5, 1.0, 0.7 and 0.5 ns.

the lower value of an order parameter ( $S$ ) for 2'(R/S),3',5'(R/S)- $d_3$ -thymidine, and details of these studies will be published elsewhere.

The above study has been subsequently extended to the 12mer duplex **II** through the folding HSQC experiment with  $^{31}\text{P}$  decoupling (no  $^2\text{H}$  decoupling) to observe the splitting of  $^{13}\text{C}(2')$  in the F1 dimension due to  $^2\text{H}$  coupling [Fig. 4(B1)]. This experiment shows that the triplet pattern for  $^{13}\text{C}(2')$ - $^2\text{H}$  coupling is clearly visible at natural  $^{13}\text{C}$  abundance, which is evident from the projection through the  $^1\text{H}$ - $^{13}\text{C}$  cross-peak in the F1 dimension [Fig. 4(B2)]. The observation of  $^{13}\text{C}(2')$ - $^2\text{H}$  splitting shows that the  $T_1$ -minimum has not been reached till 298 K for duplex **II**, which semiquantitatively allows us to define the upper limit of the overall correlation time. In this particular case, it is 4–5 ns. Clearly, more quantitative determination of the correlation times can be obtained by the simulation of the triplet pattern according to the literature procedure.<sup>6e,f</sup> Thus, the measurement of the correlation time and the relaxation parameters of any specific part in the DNA duplex, which has a selective deuterium labelling at natural  $^{13}\text{C}$  abundance [2'- and/or 5'-methylene C( $^1\text{H}$ , $^2\text{H}$ ) part], can be extracted from the line-fitting of the  $^{13}\text{C}$  splitting as well as from the  $T_1$  (and  $T_2$ ) measurement of the filtered  $^{13}\text{C}$  as mentioned above at a duplex concentration of around 2.5 mM.

## Conclusions

(1) It has been shown here that it is possible to obtain relaxation data from a specific part in an oligo-DNA at natural  $^{13}\text{C}$

abundance at a concentration of 1.13 mM. This can be easily achieved at natural abundant  $^{13}\text{C}$  provided the methylene [ $^1\text{H}$ - $^{13}\text{C}(2')$ - $^2\text{H}$ ] group in the sugar moiety is selectively deuterium labelled, without limiting the sensitivity of the HSQC experiment.

(2) In this work, we have been also able to extract the splitting pattern of  $^{13}\text{C}(^1\text{H})$  from the  $^1\text{H}(2'')$ - $^{13}\text{C}(2')$  cross-peak with  $^{13}\text{C}$  at natural abundance at 2.5 mM concentration (which is still below the aggregation concentration of the duplex) which provides an opportunity to obtain dynamic information on DNA.<sup>6</sup> Clearly, the sensitivity of the folding HSQC experiment in Fig. 4 at 2.5 mM was not adequate with the presence of 50 atom%  $^1\text{H}/^2\text{H}$  at C5' in duplex **II** because the effective  $^1\text{H}$  concentrations at C2' and C5' in duplex **II** are 2.1 and 1.25 mM, respectively. Furthermore, the H5'/5'' resonances are nearer to the water resonance than the chemical shift of H2'/2'', which reduces the signal to noise ratio for the cross-peaks between H5'/5'' and C5' much more than for the H2'/2''-C2' cross-peak. Thus our work shows that the increase of the concentration of the oligo-DNA is not the answer for the enhancement of the sensitivity of the HSQC experiment at natural abundance of  $^{13}\text{C}$ . The only way we can enhance the sensitivity of detection of both C2' and C5 at natural  $^{13}\text{C}$  abundance is to substitute one of the methylene protons at C2' or C5' with deuterium stereospecifically, which is in progress in this lab.

(3) Determination of  $^3J_{\text{H}^1\text{P}-^{13}\text{C}(2')}$  coupling constants makes it possible to distinguish between B<sub>I</sub> and B<sub>II</sub> types of sugar conformation of DNA.<sup>15</sup>

(4) The  $T_1$  relaxation rates of specific carbons are useful to understand differential dynamic properties across the DNA molecule. The  $T_1$  measurement of C2'( $^2\text{H}$ ) is also useful to extract the overall correlation times. The measurement of the correlation times together with the  $^3J_{\text{H}^1\text{P}-^{13}\text{C}(2')}$  coupling constants, increased number of nOe constraints (308 for duplex **II** whereas they are only 188 for the natural counterpart<sup>2</sup>) and homonuclear vicinal couplings obtained due to stereospecific deuterium incorporation in the sugar moieties of constituent nucleosides<sup>2</sup> improves the quality of the structure elucidation of DNA duplex by increasing the number of NMR constraints. Clearly, this set of NMR constraints can be further improved by extracting the  $T_1$  of C5'( $^2\text{H}$ ) and  $^3J_{\text{H}^1\text{P}-^{13}\text{C}(5')}$  from an appropriately labelled oligo-DNA.

## Acknowledgements

The authors thank the Swedish Board for Technical and Engineering Research (TFR), the Swedish Natural Science Research Council (NFR contract # K-KU 12067-300 to AF and K-AA/Ku04626-321 to JC) and the Wallenbergsstiftelsen for generous financial support.

## References

- 1 (a) A. Földesi, F. P. R. Nilson, C. Glemarec, C. Gioeli and J. Chattopadhyaya, *Tetrahedron*, 1992, **48**, 9033; (b) A. Földesi, F. P. R. Nilson, C. Glemarec, C. Gioeli and J. Chattopadhyaya, *J. Biochem. Biophys. Methods*, 1993, **26**, 1; (c) S.-i. Yamakage, T. V. Maltseva, F. P. R. Nilson, A. Földesi and J. Chattopadhyaya, *Nucleic Acids Res.*, 1993, **21**, 5005; (d) P. Agback, T. V. Maltseva, S.-i. Yamakage, F. P. R. Nilson, A. Földesi and J. Chattopadhyaya, *Nucleic Acids Res.*, 1994, **22**, 1404; (e) A. Földesi, S.-i. Yamakage, T. V. Maltseva, F. P. Nilson, P. Agback and J. Chattopadhyaya, *Tetrahedron*, 1995, **51**, 10 065; (f) A. Földesi, S.-i. Yamakage, F. P. R. Nilsson, T. V. Maltseva and J. Chattopadhyaya, *Nucleic Acids Res.*, 1996, **24**, 1187; (g) C. Glemarec, J. Kufel, A. Földesi, T. Maltseva, A. Sandström, L. A. Kirsebom and J. Chattopadhyaya, *Nucleic Acids Res.*, 1996, **24**, 2022; (h) E. Kawashima, K. Toyama, K. Ohshima, M. Kainosho, Y. Kyogoku and Y. Ishido, *Tetrahedron Lett.*, 1995, **36**, 6699; (i) Y. Oogo, M. A. Ono, S.-i. Tate, A. S. Ono and M. Kainosho, *Nucleic Acids Symp. Ser. 37*, 1997, 35; (j) A. Ono, T. Makita, S.-i. Tate, E. Kawashima, Y. Ishido and M. Kainosho, *Magn. Reson. Chem.*, 1996, **34**, S40; (k) S.-i. Tate, Y. Kubo, A. Ono

- and M. Kainosho, *J. Am. Chem. Soc.*, 1995, **117**, 7277; (l) C. Kojima, E. Kawashima, K. Toyama, K. Ohshima, Y. Ishido, M. Kainosho and Y. Kyogoku, *J. Biomol. NMR* **11**, 1998, 103; (m) E. Kawashima, Y. Aoyama, T. Sekine, M. Miyahara, M. F. Radwan, E. Nakamura, M. Kainosho, Y. Kyogoku and Y. Ishido, *J. Org. Chem.*, 1995, **60**, 6980; (n) A. (M.) Ono, A. Ono and M. Kainosho, *Tetrahedron Lett.*, 1997, **38**, 395; (o) A. (M.) Ono, T. Shiina, A. Ono and M. Kainosho, *Tetrahedron Lett.*, 1998, **39**, 2793; (p) X. Huang, P. Yu, E. LeProust and X. Gao, *Nucleic Acids Res.*, 1997, **25**, 4758; (q) T. J. Tolbert and J. R. Williamson, *J. Am. Chem. Soc.*, 1996, **118**, 7929; (r) J. J. De Voss, J. J. Hangeland and C. A. Townsend, *J. Org. Chem.*, 1994, **59**, 2715; (s) E. P. Nikonowicz, M. Michnicka and E. DeJong, *J. Am. Chem. Soc.*, 1998, **120**, 3813; (t) J. M. Louis, R. G. Martin, G. M. Clore and A. M. Gronenborn, *J. Chem. Biol.*, 1998, **273**, 2374; (u) T. J. Tolbert and J. R. Williamson, *J. Am. Chem. Soc.*, 1997, **119**, 12 100; (v) S. Quant, R. W. Wechselberger, M. A. Wolter, K.-H. Wörner, P. Schell, J. W. Engels, C. Griesinger and H. Schwalbe, *Tetrahedron Lett.*, 1994, **35**, 6649; (w) L. A. Agrofoglio, J.-C. Jacquinet and G. Lancelot, *Tetrahedron Lett.*, 1997, **38**, 1411; (x) A. S. Serianni and P. B. Bondo, *J. Biomol. Struct. Dyn.*, 1994, **11**, 1133.
- 2 (a) A. Földesi, T. V. Maltseva and J. Chattopadhyaya, *Tetrahedron*, 1998, **54**, 14487; (b) T. V. Maltseva, A. Földesi and J. Chattopadhyaya, *Tetrahedron*, 1998, **54**, 14528.
- 3 T. V. Maltseva, A. Földesi and J. Chattopadhyaya, *Magn. Reson. Chem.*, 1998, **36**, 227.
- 4 (a) B. H. Robinson and G. P. Drobny, *Methods Enzymol.*, 1995, **261**, 451; (b) T. M. Alam, J. Orban and G. P. Drobny, *Biochemistry*, 1991, **30**, 9229; (c) W.-C. Huang, J. Orban, A. Kintanar, B. R. Reid and G. P. Drobny, *J. Am. Chem. Soc.*, 1990, **112**, 9059; (d) R. Brandes, R. R. Vold, D. R. Kearns and A. Rupprecht, *Biochemistry*, 1990, **29**, 1717; (e) S. Roy, Y. Hiyama, D. Torchia and J. S. Cohen, *J. Am. Chem. Soc.*, 1986, **108**, 1675; (f) D. G. Brown, M. S. Sanderson, E. Garman and S. Neidle, *J. Mol. Biol.*, 1992, **226**, 481.
- 5 (a) H. P. Spielmann, *Biochemistry*, 1998, **37**, 5426; (b) P. N. Borer, S. R. LaPlante, A. Kumar, N. Zanatta, A. Martin, A. Hakkinen and G. C. Levy, *Biochemistry*, 1994, **33**, 2441; (c) S. R. LaPlante, N. Zanatta, A. Hakkinen, A. H.-J. Wang and G. C. Levy, *Biochemistry*, 1994, **33**, 2430.
- 6 (a) R. E. London, D. M. LeMaster and L. G. Werbelow, *J. Am. Chem. Soc.*, 1994, **116**, 8400; (b) L. G. Werbelow and R. E. London, *Concepts Magn. Reson.*, 1996, **8**, 325; (c) S. Grzesiek and A. Bax, *J. Am. Chem. Soc.*, 1994, **116**, 10 196; (d) J. Boyd, T. K. Mal, N. Soffe and L. D. Campbell, *J. Magn. Reson.*, 1997, **124**, 61; (e) J. F. Martin, R. L. Vold and R. R. Vold, *J. Magn. Reson.*, 1983, **51**, 164; (f) S. A. Gabel, L. A. Luck, L. G. Werbelow and R. E. London, *J. Magn. Reson.*, 1997, **128**, 101.
- 7 (a) A. J. Shaka, P. B. Barker and R. Freeman, *J. Magn. Reson.*, 1985, **64**, 547; (b) A. J. Shaka, J. Keeler, T. Frenkiel and R. Freeman, *J. Magn. Reson.*, 1983, **52**, 335.
- 8 G. Bodenhausen and D. J. Ruben, *Chem. Phys. Lett.*, 1980, **69**, 185.
- 9 (a) L. E. Kay, T. E. Bull, L. K. Nicholson, C. Griesinger, H. Schwalbe, A. Bax and D. A. Torchia, *J. Magn. Reson.*, 1992, **100**, 538; (b) L. K. Nicholson, L. E. Kay, D. M. Baldisseri, J. Arango, P. E. Young, A. Bax and D. A. Torchia, *Biochemistry*, 1992, **31**, 5253.
- 10 (a) A. G. Palmer III, M. Rance and P. E. Wright, *J. Am. Chem. Soc.*, 1991, **113**, 4371; (b) L. K. Nicholson, L. E. Kay, D. M. Baldisseri, J. Arango, P. Young, A. Bax and D. A. Torchia, *Biochemistry*, 1992, **31**, 5253.
- 11 A. Bax, M. Ikura, L. E. Kay, D. A. Torchia and R. Tschudin, *J. Magn. Reson.*, 1990, **86**, 304.
- 12 (a) L. G. Werbelow, *J. Chem. Phys.*, 1979, **70**, 5381; (b) L. G. Werbelow, *J. Chem. Phys.*, 1996, **104**, 3457; (c) L. G. Werbelow and R. E. London, *J. Chem. Phys.*, 1995, **102**, 5181; (d) L. G. Werbelow, *Understanding Chem. React.*, 1994, **8**, 223; (e) L. G. Werbelow, *J. Magn. Reson.*, 1986, **67**, 66; (f) L. G. Werbelow and A. Thevand, *J. Magn. Reson.*, 1993, **105**, 88; (g) D. T. Browne, G. L. Kenyon, E. L. Packer, H. Sternlicht and D. M. Wilson, *J. Am. Chem. Soc.*, 1973, **95**, 1316.
- 13 D. M. Kushlan and D. M. LeMaster, *J. Am. Chem. Soc.*, 1993, **115**, 11 026.
- 14 P. Schmieder, J. H. Ippel, H. van den Elst, G. A. van der Marel, J. H. van Boom, C. Altona and H. Kessler, *Nucleic Acids Res.*, 1992, **20**, 4747.
- 15 T. Szyperski, A. Ono, C. Fernandez, H. Iwai, S.-i. Tate, K. Wüthrich and M. Kainosho, *J. Am. Chem. Soc.*, 1997, **119**, 9901.

Paper 8/05708G